New Flexible Low-Density Metallic Materials Containing the (BEDT-TTF) 2 (I x Br 1- x) 3 Molecular Metals as Active Components

ARTICLE *in* THE JOURNAL OF PHYSICAL CHEMISTRY B · NOVEMBER 2001

Impact Factor: 3.3 · DOI: 10.1021/jp011470y

New Flexible Low-Density Metallic Materials Containing the $(BEDT\text{-}TTF)_2(I_xBr_{1-x})_3$ Molecular Metals as Active Components

Elena Laukhina,*,†,‡,§ Vladeslava Tkacheva,‡ Igor' Chuev,‡ Eduard Yagubskii,‡ Jose Vidal-Gancedo,† Marta Mas-Torrent,† Concepció Rovira,*,† Jaume Veciana,† Salavat Khasanov,*,|| Roman Wojciechowski,⊥ and Jacek Ulanski⊥

Institut de Ciencia de Materials de Barcelona, CSIC, Campus UAB, E-08193 Bellaterra, Spain, IPCP RAS, 142432, Chernogolovka, MD, Russia, ISSP RAS, 142432, Chernogolovka, MD, Russia, and Department of Molecular Physics, Technological University of Lodz, 90-924, Lodz, Poland

Received: April 18, 2001; In Final Form: August 15, 2001

New conducting bilayer films (BL-film) containing $(BEDT\text{-}TTF)_2(I_xBr_{1-x})_3$ molecular metals as active components have been prepared. The effect of various parameters of the BL-film preparation on the conducting layer composition was systematically studied by X-ray, Raman, EPR, and SEM. It was shown that the conducting layer of new BL-films is formed by "*c*" oriented $(BEDT\text{-}TTF)_2(I_xBr_{1-x})_3$ nanocrystals which contain a set of the IBr_2^-, I_2Br^-, and/or I_3^- anions. It was found that the $\alpha' \rightarrow \beta$ phase transition takes place in the $(BEDT\text{-}TTF)_2(I_xBr_{1-x})_3$ nanocrystals under film annealing. Some of the new composite BL-films, being flexible and transparent, reveal a metal-like temperature dependence of resistance down to nitrogen temperature.

1. Introduction

Polymeric composite films[1−4] containing a thin layer of organic conductors are very attractive as conducting materials for a novel generation of devices which can gain the unusual electronic properties of molecular metals.[5] These composite bilayer (BL) films demonstrate different transport properties[1,6,7] retaining the advantageous properties of the polymeric matrix such as flexibility, transparency and low density. We have reported an unique BL-film featuring a metallic behavior of resistance over the whole temperature range studied and revealing superconducting properties below 5−7 K.[1,8] This material contains a conducting surface layer formed by the linked microcrystals of the organic superconductor β_t-$(BEDT\text{-}TTF)_2I_3$ (BEDT-TTF = bis(ethylenedithio)tetrathiafulvalene).[9,10] Other flexible and transparent BL-films with a very thin conducting surface layer of BET/I_3,[3] $(BEDO\text{-}TTF)_{2.4}I_3$, or β-$(BEDO\text{-}TTF)_2Br{\cdot}3H_2O$[6] microcrystals (BET-TTF = bis(ethylenethio)tetrathiafulvalene; BEDO-TTF = bis(ethylenedioxo)tetrathiafulvalene) also demonstrate metal-like transport properties in a wide temperature region. The above BL-films can be successfully prepared by the modified reticulate doping technique (MRDT).[1,4,8] During the progress of our research, we have extended the MRDT for the preparation of new conducting BL-films with a conducting surface layer formed by nanocrystals of $(BEDT\text{-}TTF)_2(I_xBr_{1-x})_3$ molecular metals. These new transparent flexible films are conductors in a wide temperature region, some of them revealing a metal-like behavior of resistance down to nitrogen temperature.

Here we present the preparation of new conducting BL-films containing $(BEDT\text{-}TTF)_2(I_xBr_{1-x})_3$ molecular conductors as active components and the effect of various conditions of MRDT on the structure and texture of the $(BEDT\text{-}TTF)_2(I_xBr_{1-x})_3$ conducting layers. Additionally, the details of the $\alpha' \rightarrow \beta$ structural phase transition of the new $(BEDT\text{-}TTF)_2(I_xBr_{1-x})_3$ molecular conductors under film annealing and the transport properties of all new conducting BL-films in a wide temperature region are also outlined in this paper.

2. Experimental Section

A. Film Preparation. Polycarbonate (PC) films (10−15 μm thickness) containing 2 wt % of molecularly dispersed BEDT-TTF were made by casting the solution of PC (≅1 g) and BEDT-TTF (0.02 g) in 1,2-dichlorobenzene (≈50 mL) at t = 130 °C as previously described[2,7] (first stage, Scheme 1). Then the

SCHEME 1: Scheme of MRDT Used for the Preparation of New Conducting BL-Films with the Conducting Layer of the β_t-$(BEDT\text{-}TTF)_2(I_xBr_{1-x})_3$ Nanocrystals

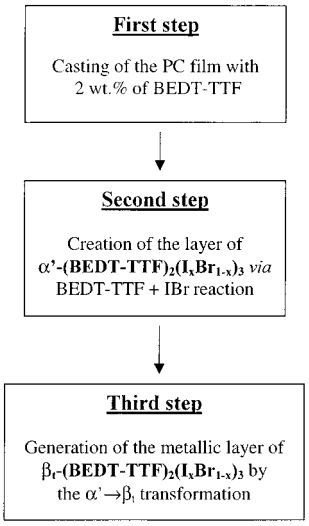

* To whom correspondence should be addressed. ICMAB Campus UAB, E-08193 Bellaterra, Spain. FAX: (34)93 580 57 29. E-mail: vladimir@icmab.es and cun@icmab.es.
† Institut de Ciencia de Materials de Barcelona.
‡ IPCP RAS.
§ Permanent address: IPCP RAS, 142432, Chernogolovka, MD, Russia.
|| ISSP RAS.
⊥ Department of Molecular Physics.

10.1021/jp011470y CCC: $20.00
Published on Web 10/23/2001

TABLE 1: Parameters of the Second Step Used for the Film Samples Preparation

film sample	temp, °C	$C_{IBr/s}$, M	time period of the treatment, min
1	23	0.024	2
2	23	0.024	4
3	23	0.024	6
4	23	0.024	10
5	25	0.036	2
6	25	0.036	4
7	25	0.036	6
8	23	0.048	2
9	23	0.048	4
10	23	0.048	6

surface of the PC/ BEDT-TTF film was treated with vapor of a IBr/CH_2Cl_2 solution during different time periods (Table 1), which provided a way to form a conducting surface layer with the α′-$(BEDT\text{-}TTF)_2(I_xBr_{1-x})_3$ nanocrystals (second step, Scheme 1). During the second step we used a binary mixture system: IBr/CH_2Cl_2 solution−IBr/CH_2Cl_2 vapor at equilibrium. The mole fraction of IBr contained in a IBr/CH_2Cl_2 solution (x^*_{IBr}) was always much greater than the mole fraction of BEDT-TTF ($x^*_{BEDT-TTF}$) contained in the swollen surface layer of the film. All time periods used for the film surface treatment were not sufficient to achieve the saturation of the swollen layer of the film with IBr. Afterward, all the BL-films were annealed at 155−160 °C during 3 h to form the β_t-$(BEDT\text{-}TTF)_2(I_xBr_{1-x})_3$ conducting layer (third step, Scheme 1). To prevent a degradation of the nanocrystals during the BL-film annealing, the conducting surface of the film samples has to be protected sandwiching them between two glass plates. To provide a protective coat for the conducting surface layer, we also successfully used an aluminum foil.

B. BL-Film Characterization. X-ray diffraction patterns have been measured using Siemens D-500 diffractometer in the reflection mode.

The Raman spectra of the composite films were recorded at room temperature using Jobin-Yvon T64000 MicroRaman spectrometer, working in a backscattering mode. The measurements were performed with 632 nm laser line and with spectral resolution of 1 cm^{-1}. Diamond (1332 cm^{-1}) and silicon (520 cm^{-1}) lines were used for the calibration of the spectrometer. Two typical Raman spectra of the film samples are depicted in Figure 1.

EPR spectra were recorded using Bruker WSP-300E spectrometer operating in the X-band (9.5 GHz) with a rectangular TE 102 cavity and equipped with a field-frequency (F/F) lock accessory and a built-in Bruker NMR gaussmeter ER 035 M. Heating was made with a rate of 1°/min in a Bruker ER 4121 HT nitrogen cryostat (100−500 K) (see Figure 2.) Rotations were performed by means of a Bruker programmable goniometer ER 218 PGl 8 (see Figure 3). Precautions to avoid undesirable spectral line broadening, such as that arising from microwave power saturation and magnetic field overmodulation, were taken.

The morphology of conducting surface layers was investigated using a scanning electron microscope (SEM) operating at 20 kV. The SEM micrographs of BL films **1**, **7**, and **8** are presented in Figure 4.

Temperature resistance dependencies were measured down to 1.5 K using a standard 4-probe dc-method. Four annealed platinum wires (20 μm in diameter) were attached to the conducting surface of a BL-film by a conductive graphite paste. The scheme of a film sample montage is presented as an insert of Figure 5.

3. Results and Discussion

To gain a better understanding of the possibilities and restrictions of MRDT, it is very important to clarify the real processes that take place during the BL-film preparation. Thus, what kind of conducting nanocrystals can be formed at the second step via BEDT-TTF + IBr reaction is certainly a question to answer. Undoubtedly, the thermodynamic consideration of the BEDT-TTF + IBr reaction have to be useful to clarify the problem.

A. Chemical Reactions Due to the BEDT-TTF and IBr Interaction. Ab Initio Estimation and Effect of the Experimental Parameters. Below we will focus on the consideration of chemical reactions which can occur in the swollen surface layer of the PC/BEDT-TTF film at the second step of MRDT (Scheme 1). Assuming that the nanocrystals of the conducting layer are formed under a steady chemical reaction, we can estimate the probability P of each plausible BEDT-TTF + IBr reaction on the basis of Boltzmann distribution $p \sim \exp(-E/RT)$, where E is energy, R is the universal gas constant, and T is temperature. The analysis of all the possible results of the BEDT-TTF + IBr interaction producing species such as $I^{\pm1,0}$, $I_2^{\pm1,0}$, $I_3^{\pm1,0}$, $IBr^{\pm1,0}$, $Br^{\pm1,0}$, $Br_2^{\pm1,0}$, $Br_3^{\pm1,0}$, $IBr_2^{\pm1,0}$, and $I_2Br^{\pm1,0}$, allows us to restrict the set of the most energetically favorable reactions, which result in the maximum (2-fold) enhancement of the number of new bonds, by a factor of five:

$$8BEDT\text{-}TTF + 6IBr \leftrightarrow [8(BEDT\text{-}TTF)]^{+4} + 2I_2Br^- + 2IBr_2^- \quad (1)$$

$$8BEDT\text{-}TTF + 6IBr \leftrightarrow [8(BEDT\text{-}TTF)]^{+4} + I_3^- + 3IBr_2^- \quad (2)$$

$$8BEDT\text{-}TTF + 6IBr \leftrightarrow [8(BEDT\text{-}TTF)]^{+4} + Br_3^- + 3I_2Br^- \quad (3)$$

$$8BEDT\text{-}TTF + 6IBr \leftrightarrow [8(BEDT\text{-}TTF)]^{+4} + 2I_3^- + 2Br_3^- \quad (4)$$

$$8BEDT\text{-}TTF + 6IBr \leftrightarrow [8(BEDT\text{-}TTF)]^{+4} + I_3^- + I_2Br^- + IBr_2^- + Br_3^- \quad (5)$$

The energy of the reactions was calculated on the basis of an additive approach. It means that intermolecular interactions of the reagents were not taken into consideration. For all these reactions, we have compared only the energies of the species formed due to the reduction of IBr, since the contributions of the others species are constant. Ab initio calculations (Table 2) have been carried out on the MP2/LANL2DZ level (GAUSSIAN94).[11] The effect of the solvent (nitrobenzene) was calculated according to the Onsager model.[12] We were especially interested in the estimation of the effect of nitrobenzene since we had already found that the β-type crystals which were synthesized in nitrobenzene via BEDT-TTF + IBr reaction[13] contain the assembly of I_3^-, I_2Br^-, and IBr_2^- anions.[14] On the basis of the calculations tabled in Table 2, the probability of the reactions 3−5 equals zero. Thus, for the BEDT-TTF + IBr reaction (second step of MRDT), it would be plausible to suggest the formation of the I_3^-, I_2Br^-, and IBr_2^- trihalide anions only. We have also estimated the contribution of each of these trihalide anions in vacuum and nitrobenzene. These data are summarized in Table 3. According to these results, the anion composition of the above-mentioned single crystals obtained in nitrobenzene can be formulated as $[(I_3)_{0.07}(I_2Br)_{0.37}(IBr_2)_{0.56}]^-$

TABLE 2: Energy of Changing Species *E* in the Proposed BEDT-TTF + IBr Reaction and Boltzmann Probability *P* of This Reaction in Vacuum (v) and in Nitrobenzene (s)

reaction	E_v, au	P_v	E_s, au	P_s
1	−145.250	0.5	−145.339	0.74
2	−145.250	0.5	−145.338	0.26
3	−145.237	0	−145.318	0
4	−145.224	0	−145.294	0
5	−145.237	0	−145.317	0

TABLE 3: Contribution *C* of Trihalide Anions in Vacuum (v) and in Nitrobenzene (s)

anion	C_v,%	C_s,%
I_3^-	12.5	6.5
I_2Br^-	25.0	37.0
IBr_2^-	62.5	56.5

that gives us an average stoichiometry of $I_{1.5}Br_{1.5}$ for the anion. This result is in excellent agreement with EDX data which indicate for this compound the I/Br atomic ratio of 1:1.[13]

In line with the thermodynamic consideration (Tables 2 and 3), one can expect with reasonable confidence that the contribution of each trihalide anion should be different in various organic solvents and depend on the polarity of the environment. Since the polarity of a swollen polymeric matrix depends on different factors (amount of 1,2-dichlorobenzene used at the first step, variation of CH_2Cl_2 concentration with time at the second step and polarity of PC), the contribution of each trihalide anion to the composition of the nanocrystals that form the conducting layers is difficult to estimate quantitatively. Nevertheless, in accordance with the ab initio calculations, we may presume that in the swollen surface of the BL-film samples the $(BEDT\text{-}TTF)_2(I_xBr_{1-x})_3$ nanocrystals containing the majority of the IBr_2^- anions along with smaller amounts of the I_3 and/or I_2Br^- species should be mainly formed. In attempting to estimate the *x* value in the outlined formula, one should also keep in mind that the size of trihalide anions sets limits on the formation of different crystal phases of the BEDT-TTF trihalide family. For example, I_3^- species promote the formation of α-, *β*-, *θ*-, and *κ*-type crystal modifications of the $(BEDT\text{-}TTF)_2I_3$ salt, while smaller IBr_2^- species are beneficial for α′- and *β*-type $(BEDT\text{-}TTF)_2IBr_2$ crystal phases only.[5] Therefore, at the second step via BEDT-TTF + IBr reaction the α′-$(BEDT\text{-}TTF)_2(I_xBr_{1-x})_3$ and/or *β*-$(BEDT\text{-}TTF)_2(I_xBr_{1-x})_3$ crystal phases can be expected to form along with other above crystal modifications. Some amount of amorphous salts with mixed anions can be also formed. Considering all this, the *x* value should depend on the type of the crystal phase and may differ for various nanocrystals. Evidently, to characterize the conducting layer of new BL-film samples, we should determine the type of nanocrystals (BEDT-TTF packing motif) and the composition of the anion as well. We have chosen X-ray, EPR, and Raman spectroscopy as the techniques for the films' characterization, which are the best suited for both outlined requirements.

The reagent ratio at the BEDT-TTF + IBr reaction is also a very important parameter because it determines the formation of trihalide salts with a different charge-transfer degree. We suggest that there is a range of optimum masses of IBr absorbed per unit volume of a swollen film surface layer ($C_{IBr/film}$) at which a conducting layer of $(BEDT\text{-}TTF)_2(I_xBr_{1-x})_3$ nanocrystals is achieved. Generally, the $C_{IBr/film}$ value is proportional to (i) the mass of IBr in the vapors of IBr/CH_2Cl_2 solution ($m_{IBr/v}$) and (ii) the duration of the film surface treatment *t*. According to the gas-state equations[15] and by Henry's law,[15] the $m_{IBr/v}$ value is proportional to the mole fraction of IBr (x_{IBr}*) contained in the IBr/CH_2Cl_2 solution and it can be shown that

$$C_{IBr/film} \cong D_{IBr} C_{IBr/s} V_s t \quad (1)$$

where D_{IBr} is the capability of IBr vapors to penetrate into a swollen polycarbonate layer, $C_{IBr/s}$ is the molar concentration of IBr, and V_s is the volume of IBr/CH_2Cl_2 solution. To find the above range of the $C_{IBr/film}$ optimum values we varied $C_{IBr/s}$ and *t* values (see Table 1); in all experiments the amount of BEDT-TTF, the treated film surface layers (7 cm^2), volumes of vapor (29.5 mL), and solution (10.5 mL) were identical. The second steps were done at the same temperature to fix the following parameters: D_{IBr} values, rate of the reaction, and rate of the reagents' diffusion. Taking into account the outlined particularities of the second step of MRDT, we may restrict ourselves to the simple estimation of the $C_{IBr/film}$ values with the factor F_{IBr} that is proportional to the molar concentration of IBr in CH_2Cl_2 and duration of a film surface treatment (Table 1):

$$F_{IBr} = C_{IBr/s} t \quad (2)$$

By using different concentrations of IBr in IBr/CH_2Cl_2 solutions ($C_{IBr/s}$) and various time periods of a surface treatment, we have prepared different BL-film samples **1**−**10** (Table 1). These conducting BL-films were eventually formed with different F_{IBr} values.

B. Composition and Structure of Conducting Layers after the Second Step of the Film Preparation. The X-ray analysis of BL-film samples indicate the presence in all spectra of only (00*l*) reflections that are characteristic of conducting layers formed by oriented nanocrystals. The *c** axis of the nanocrystals is perpendicular to the film surface and, consequently, their conducting layers are parallel to it. The measured values of the interplanar spacing d_{001} along with intensities of (00*l*) reflections allowed us to identify the different phases of the BEDT-TTF trihalides (Table 4).

While at the highest values of F_{IBr} (film samples **4**, **7**, **9** and **10**) the most intensive reflections correspond to the α′-$(BEDT\text{-}TTF)_2IBr_2$ phase with d_{00l} = 16.32 Å, at the lower F_{IBr} values (film samples **1**−**3**, **5**, **6**, and **8**) the most intensive reflections indicate the existence of the α′ phases with the characteristic values of d_{001} in the range from 16.365(3) to 16.422(3) Å. Since these d_{001} values are higher than those of the α′-$(BEDT\text{-}TTF)_2IBr_2$ single crystal, it may be suggested that the conducting layer of samples **1**−**3**, **5**, **6**, and **8** consists of α′-type nanocrystals with an anion layer which should contain the IBr_2^- species along with bigger trihalide anions such as I_3^- and/or I_2Br^-. Thus, X-ray data show that the conducting layer of BL-films produced at the lowest F_{IBr} values consists of the α′-$(BEDT\text{-}TTF)_2(I_xBr_{1-x})_3$ nanocrystals ($0.66 > x > 0.33$) containing different sets of the IBr_2^-, I_2Br^-, and I_3^- trihalide anions. These X-ray data are in agreement with the thermodynamic consideration of the BEDT-TTF + IBr interaction (see above). It should be noted that the X-ray diffraction patterns of samples **2**, **3** also demonstrate extra small reflections corresponding to the *β* phase of BEDT-TTF salts.[5,13] In the X-ray diffraction patterns of samples **3**, **4**, **9**, and **10** the extra reflections correspond to a new BEDT-TTF trihalide salt (N-salt) with d_{001} = 33.30(1) Å (Table 4). While according to X-ray data the metallic *β*-$(BEDT\text{-}TTF)_2(I_xBr_{1-x})_3$ nanocrystals with the value of *x* equal to 0.70(5) (sample **2**) or 0.61(5) (sample **3**) are formed in a small amount, the contribution of the N-salt can be significant especially in the BL-film samples prepared at the highest F_{IBr} values (F_{IBr} = 24 M min, sample **4**, and F_{IBr} = 28.8 M min, sample **10**). The formation of the N-salt is undesirable from the viewpoint of the electrical properties of

TABLE 4: Composition of the Conducting Layer of the Films after the Second Step of the Film Preparation

sample	F_{IBr} 10^{-2}, M min	X-ray data			conducting layer composition[a]
		d_{00l}, Å	phase	$(I_xBr_{1-x})_3$	
			At $C_{IBr/s}$ = 0.024 M		
1	4.8	16.402(3)	α′	$0.66 > x > 0.33$	α′-(BEDT-TTF)$_2$(I$_3$)$_y$ (I$_2$Br)$_z$(IBr$_2$)$_{1-y-z}$
2	9.6	16.407(3)	α′	$0.66 > x > 0.33$	α′-(BEDT-TTF)$_2$(I$_3$)$_y$(I$_2$Br)$_z$(IBr$_2$)$_{1-y-z}$
		15.04(1)	β	$x = 0.70(5)$	β-(BEDT-TTF)$_2$(I$_3$)$_y$ (I$_2$Br)$_z$(IBr$_2$)$_{1-y-z}$
		16.365(3)	α′	$0.66 > x > 0.33$	
3	14.4	15.02(1)	β	$x = 0.61(5)$	α′-(BEDT-TTF)$_2$(I$_3$)$_y$ (I$_2$Br)$_z$(IBr$_2$)$_{1-y-z}$,
		33.32(1)	new		β-(BEDT-TTF)$_2$(I$_3$)$_y$ (I$_2$Br)$_z$(IBr$_2$)$_{1-y-z}$
					N-salt
4	24.0	16.320(5)	α′	$x = 0.33$	
		33.32(1)	new		α′-(BEDT-TTF)$_2$IBr$_2$ and
					N-salt
			At $C_{IBr/s}$ = 0.036 M		
5	7.2	16.422(2)	α′	$0.66 > x > 0.33$	α′-(BEDT-TTF)$_2$ (I$_2$Br)$_y$(IBr$_2$)$_{1-y}$
6	14.4	16.380(3)	α′	$0.66 > x > 0.33$	α′-(BEDT-TTF)$_2$ (I$_2$Br)$_y$(IBr$_2$)$_{1-y}$
7	21.6	16.325(5)	α′	$x = 0.33$	α′-(BEDT-TTF)$_2$IBr$_2$
			At $C_{IBr/s}$ = 0.048 M		
8	9.6	16.380(3)	α′	$x > 0.33$	α′-(BEDT-TTF)$_2$ (I$_2$Br)$_y$(IBr$_2$)$_{1-y}$
9	19.2	16.31(1)	α′	$x = 0.33$	
		33.26(4)	new		α′-(BEDT-TTF)$_2$IBr$_2$
					N-salt
10	28.8	16.317(4)	α′	$x = 0.33$	α′-(BEDT-TTF)$_2$IBr$_2$ and
		33.30(1)	new		N-salt

[a] The anion composition of nanocrystals was determined by Raman spectroscopy (see Table 5).

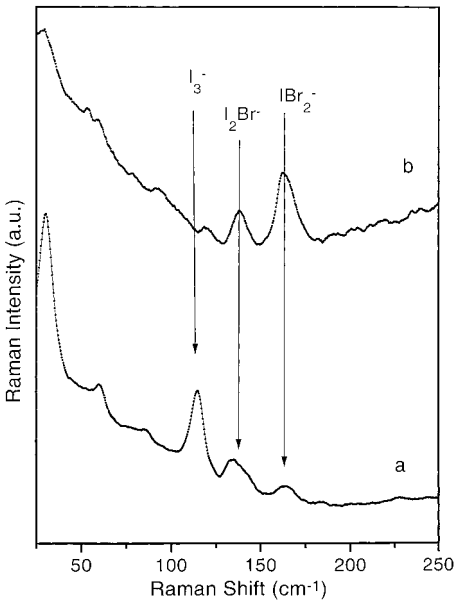

Figure 1. Raman spectra of film samples (a) **1** and (b) **7** containing the conducting layer of the α′-(BEDT-TTF)$_2$(I$_x$Br$_{1-x}$)$_3$ nanocrystals.

BL-films (see below). The X-ray results indicate that at the second step of MRDT via BEDT-TTF + IBr reaction two types of conducting layers can be formed: (i) conducting layers containing only α′-type nanocrystals and (ii) conducting layers consisting of different BEDT-TTF trihalide salts. Therefore, at the second step of MRDT we have a good chance to achieve the optimum $C_{IBr/film}$ value which is favorable to the generation of an uniform surface conducting layer composed of only the α′ phase of BEDT-TTF trihalide salts.

It has been demonstrated by both ab initio calculations and Raman studies of single crystals[14] that Raman spectra can be successfully used to clarify the $(I_xBr_{1-x})_3^-$ anion composition by observing the distinct halogen vibrations of the trihalide anions in the range of 100−200 cm^{-1}. Low-frequency Raman measurements were therefore performed in order to define which types of trihalide anions are included in the anion layer of the

TABLE 5: Data of Low-Frequency Raman Spectra of the BL-Film Samples with the Conducting Layer Formed during the Second Step of MRDT

BL-film sample	Raman ν, cm^{-1} [a]	assignment
1	115 s	υ^b I_3^-
	135 m	υ I_2Br^-
	164 w	υ IBr_2^-
2	115 m	υ I_3^-
	135 m	υ I_2Br^-
	164 m	υ IBr_2^-
3	115 vw	υ I_3^-
	135 m	υ I_2Br^-
	164 m	υ IBr_2^-
4	135 vw	υ I_2Br^-
	164 m	υ IBr_2^-
5	115 m	υ I_3^-
	135 m	υ I_2Br^-
	164 m	υ IBr_2^-
6	135 w	υ I_2Br^-
	164 m	υ IBr_2^-
7	135 vw	υ I_2Br^-
	164 m	υ IBr_2^-
	135 m	υ I_2Br^-
8	164 s	υ IBr_2^-
9	135 vw	υ I_2Br^-
	164 m	υ IBr_2^-
10	164 m	υ IBr_2^-

[a] Relative intensities: s = strong, m = medium, w = weak, vw = very weak. [b] υ is a symbol used for stretching vibrations of a trihalide anion.

α′-, β-, and N-type nanocrystals. In this frequency range the quality of the Raman spectra of film samples studied are enough to detect Raman bands as well as to assign them to vibrations of either I_3^-, I_2Br^-, or IBr_2^- anions (Figure 1, Table 5). The low-frequency Raman spectra of samples **1**−**3** and **5** shows the band at 115 cm^{-1} due to the stretching vibration of I_3^- anions and two bands at 135 and 164 cm^{-1} resulting from the stretching vibrations of the I_2Br^- and IBr_2^- anions, respectively.[14,17] The Raman spectra of samples **4** and **6**−**9** show only the two bands of the stretching vibrations of the I_2Br^- and IBr_2^- linear anions, while the stretching vibration of sample **10** shows only a band due to the IBr_2^- species. These results are in excellent agreement

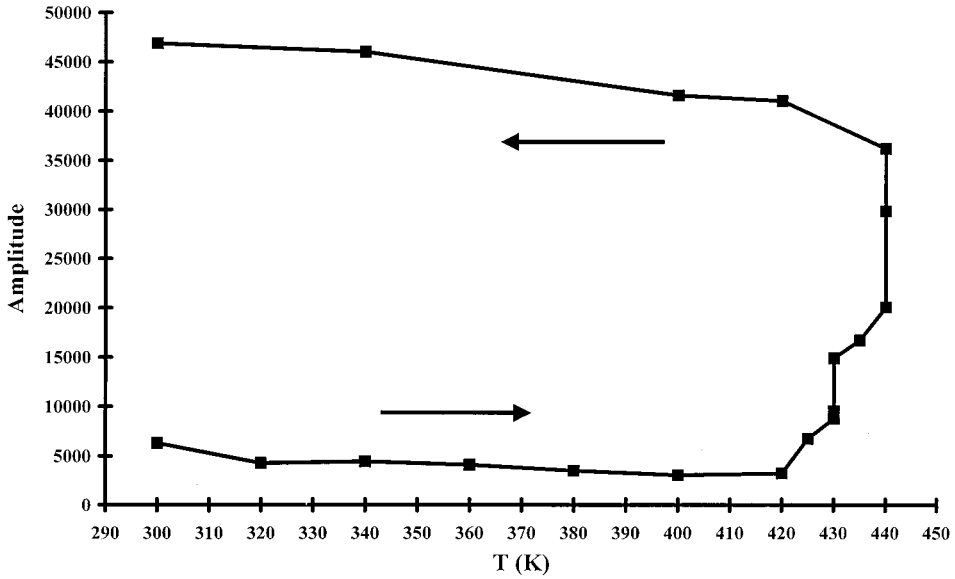

Figure 2. Temperature dependence of the EPR signal amplitude for sample **1** containing the conducting layer of the (BEDT-TTF)$_2$(I_xBr_{1-x})$_3$ nanocrystals.

with X-ray data and not contradictory to the presented thermodynamic consideration.

The quantitative analysis of the EPR signal of these BL-films, taking into account the EPR characteristics of both α′- and β-(BEDT-TTF)$_2$IBr$_2$ phases, is consistent with a very small (2−4%) amount of β-type nanocrystals in all the studied samples.

C. Structural Phase Transition at High Temperature. Taking into account that the well-known α′ → β (BEDT-TTF)$_2$IBr$_2$ phase transformation takes place at 156 °C,[18,19] we have looked for a similar structural phase transition for the new α′-(BEDT-TTF)$_2$(I_xBr_{1-x})$_3$ nanocrystals. To do so, we have studied the temperature dependence of the EPR signal of film **1** oriented perpendicular to the static magnetic field in a wide temperature region. As it was mentioned above, the EPR signal of the film samples consists of two different signals: one intensive but very broad signal of the α′-type nanocrystals with a line width (ΔH_{pp}) of 75 G and another small but narrower signal of the β phase impurity with ΔH_{pp} = 25 G. Since the observation of the temperature dependence of a broad signal is difficult, especially at high temperature, we have studied the temperature dependence of the narrow signal of the β phase impurity that has to increase during the α′ → β phase transition. The amplitude of the β phase signal was temperature independent up to 420 K (see Figure 2) and above 420 K the amplitude of the signal started to increase. A 8-fold buildup of the amplitude was observed about 440 K (Figure 2). Above 440 K the EPR signal with ΔH_{pp} = 25 G, g = 2.0070, which is characteristic of the β phases[7] (Scheme 2), becomes irreversibly dominant. This is an indication that the majority of the α′-(BEDT-TTF)$_2$(I_xBr_{1-x})$_3$ nanocrystals have been transformed to the metallic β_t-type nanocrystals.

To verify the orientation of the β_t-(BEDT-TTF)$_2$(I_xBr_{1-x})$_3$ nanocrystals which were formed during the third step, the EPR spectra of the annealed BL-film **1** in different orientations with respect to the static magnetic field were performed. The g factor variation is plotted in Figure 3. The g factor reaches a maximum when the magnetic field is perpendicular to the film plane and a minimum when it is parallel to that. This minimum g factor does not change upon rotation in the film plane. Since the maximum g value for the β-type single crystal[8] is found when the static magnetic field is parallel to the c* crystallographic axis, the above results allow us to conclude that the β_t-(BEDT-TTF)$_2$(I_xBr_{1-x})$_3$ nanocrystals are oriented with the c* axis perpendicular to the film plane. Thus, the EPR studies confirm the X-ray data (see below). In addition, the isotropic behavior found upon rotation around c* axis indicates that there is not a predominant in-plane orientation of the nanocrystals.

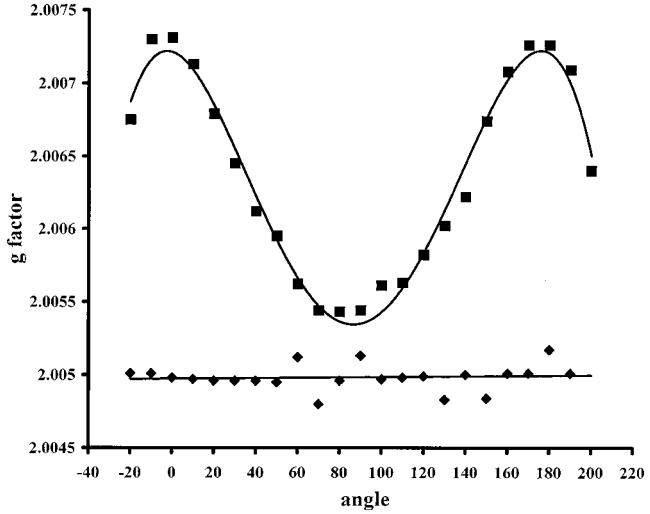

Figure 3. Angle dependence of g factor for film sample **1** containing the conducting layer of the β_t-(BEDT-TTF)$_2$(I_xBr_{1-x})$_3$ nanocrystals. (■) θ is the angle between the c* axis and the external magnetic field; (◆) rotation around the c* axis.

SCHEME 2: Schematic View of the α′ → β Structural Transformation of the BEDT-TTF Packing in the (BEDT-TTF)$_2$(I_xBr_{1-x})$_3$ Nanocrystals

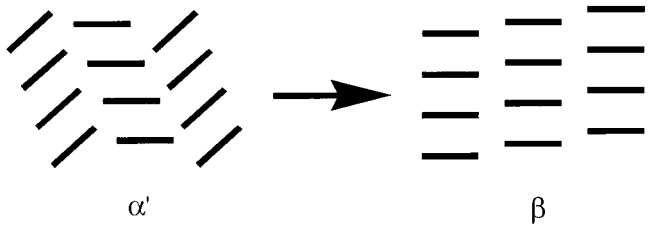

D. Composition and Structure of the BL-Film's Conducting Layers after Annealing. We have also tested all the film samples after 3 h annealing at 155−160 °C (Table 6) by X-ray

TABLE 6: Composition of the Conducting Layer of the BL-Film Samples after the Film Annealing

	X-ray data			
sample	d_{00l}, Å	phase	$(I_xBr_{1-x})_3$	conducting layer composition
1	15.038(3)	β	$x = 0.69(2)$	β-(BEDT-TTF)$_2$(I$_3$)$_y$(I$_2$Br)$_z$(IBr$_2$)$_{1-y-z}$[a]
2	15.04(1)	β	$x = 0.69(2)$	β-(BEDT-TTF)$_2$(I$_3$)$_y$(I$_2$Br)$_z$(IBr$_2$)$_{1-y-z}$
3	15.020(3)	β	$x = 0.61(3)$	β-(BEDT-TTF)$_2$(I$_3$)$_y$(I$_2$Br)$_z$(IBr$_2$)$_{1-y-z}$
4	15.01(1)	β	$x = 0.57(5)$	β-(BEDT-TTF)$_2$(I$_3$)$_y$(I$_2$Br)$_z$(IBr$_2$)$_{1-y-z}$
	16.33(1)	α'	$x = 0.33$	α'-(BEDT-TTF)$_2$IBr$_2$
	33.31(1)	new		N-salt
5	15.025(5)	β	$x = 0.63(3)$	β-(BEDT-TTF)$_2$(I$_3$)$_y$(I$_2$Br)$_z$(IBr$_2$)$_{1-y-z}$[a]
	15.013(3)	β	$x = 0.58(2)$	β-(BEDT-TTF)$_2$(I$_3$)$_y$(I$_2$Br)$_z$(IBr$_2$)$_{1-y-z}$
6	16.220(5)			BEDT-TTF
7	15.007(2)	β	$x = 0.55(2)$	β-(BEDT-TTF)$_2$(I$_3$)$_y$(I$_2$Br)$_z$(IBr$_2$)$_{1-y-z}$
8	16.31(1)	α'	$x = 0.33$	α'-(BEDT-TTF)$_2$IBr$_2$
	14.993(3)	β	$x = 0.50(2)$	β-(BEDT-TTF)$_2$ (I$_3$)$_y$(I$_2$Br)$_z$(IBr$_2$)$_{1-y-z}$
9	14.990(3)	β	$x = 0.44(2)$	β-(BEDT-TTF)$_2$(I$_3$)$_y$(I$_2$Br)$_z$(IBr$_2$)$_{1-y-z}$
	16.32(1)	α'	$x = 0.33$	α'-(BEDT-TTF)$_2$IBr$_2$
	33.32(1)	new		N-salt
10	14.995(5)	β	$x = 0.48(2)$	β-(BEDT-TTF)$_2$(I$_3$)$_y$(I$_2$Br)$_z$(IBr$_2$)$_{1-y-z}$
	16.32(1)	α'	$x = 0.33$	α'-(BEDT-TTF)$_2$IBr$_2$
	33.315(1)	new		N-salt

[a] The composition of the anion layer of these nanocrystals was found by Raman spectroscopy.

and Raman spectroscopies. In the X-ray diffraction patterns of annealed samples **1** and **5**−**7**, the reflections of the α'-(BEDT-TTF)$_2$(I$_x$Br$_{1-x}$)$_3$ phases ($0.66 > x \geq 0.33$) have disappeared. Instead, the strong reflections of a new phase arise. The d_{001} values of the reflections of annealed nanocrystals (Table 6) correspond to the β-type of the BEDT-TTF trihalide salts[8] (Scheme 2). In the case of β phases, based on the $d_{001}(x)$ composition dependence obtained from the known single-crystal cell parameters for β-(BEDT-TTF)$_2$I$_3$, β-(BEDT-TTF)$_2$I$_2$Br, and β-(BEDT-TTF)$_2$IBr$_2$, we were able to estimate the stoichiometry of the anion in the β-(BEDT-TTF)$_2$(I$_x$Br$_{1-x}$)$_3$ nanocrystals (Tables 4 and 6).

In the X-ray diffraction patterns of annealed samples **2** and **3** only intensive reflections of the β-(BEDT-TTF)$_2$(I$_x$Br$_{1-x}$)$_3$ salt with an x value of 0.70 and 0.61, respectively, are observed, and the reflections of the α'-type nanocrystals have disappeared. The X-ray diffraction patterns of annealed film samples **4** and **8**-**10** are more complicated. In the X-ray diffraction patterns of samples **4**, **9**, and **10** there are extra new reflections characteristic of the β-(BEDT-TTF)$_2$(I$_x$Br$_{1-x}$)$_3$ nanocrystals along with initial reflections of the α'-(BEDT-TTF)$_2$IBr$_2$ and N-salt. (Table 6). In the X-ray diffraction pattern of sample **8** the initial reflections of the α'-(BEDT-TTF)$_2$(I$_x$Br$_{1-x}$)$_3$ salt have disappeared. Instead, the 00l reflections of β-(BEDT-TTF)$_2$(I$_x$Br$_{1-x}$)$_3$ and α'-(BEDT-TTF)$_2$IBr$_2$ arise.

The presence of only 00l reflections of the β-type phases show that conducting layers generated during the third step consist of β_t–-type nanocrystals which are arranged just as those of the α'-type were aligned. Below let us focus on the d_{001} values corresponding to the β-type of the BEDT-TTF trihalide nanocrystals (Table 6). Experimentally, the d_{001} values of all β_t-type nanocrystals forming the conducting layer of the BL-films prepared are in the range from 14.990(3) Å to 15.04(1) Å. Since these d_{001} values are over the d_{001} value of the superconductor β-(BEDT-TTF)$_2$IBr$_2$ single crystal ($d_{001} = 14.95$ Å) and under the d_{001} value of the superconductor β-(BEDT-TTF)$_2$I$_3$ single crystal ($d_{001} = 15.109$ Å), we may conclude that, similarly to the α'-(BEDT-TTF)$_2$(I$_x$Br$_{1-x}$)$_3$ nanocrystals, the β_t-type nanocrystals contain the set of trihalide anions: IBr_2^-, I_3^-, and I_2Br^-. The X-ray data presented in Table 6 surprisingly show that at the third step of MRDT the stoichiometry of the anion layers of the (BEDT-TTF)$_2$(I$_x$Br$_{1-x}$)$_3$ nanocrystals has changed. This result is attributable to some solid-state reactions, which can take place during a BL-film annealing. For example, we have found that the decomposition of the conducting nanocrystals via reduction of BEDT-TTF$^{+\cdot}$ to a neutral molecule proceeds under the BL-films annealing (see experimental part). Therefore, it may be surmised that the $\alpha' \rightarrow \beta$ structural phase transition in the (BEDT-TTF)$_2$(I$_x$Br$_{1-x}$)$_3$ nanocrystals is probably accompanied by the following solid-state reactions:

$$\left.\begin{array}{l}\alpha'\text{-(BEDT-TTF)}_2(I_xBr_{1-x})_3\\ \beta\text{-(BEDT-TTF)}_2(I_xBr_{1-x})_3\\ \text{amorphous(BEDT-TTF)}/(I_xBr_{1-x})_3\end{array}\right\} \rightarrow \text{BEDT-TTF} + \text{IBr} \rightleftharpoons \begin{cases}\alpha'_t\text{-(BEDT-TTF)}_2\text{IBr}_2\\ \beta_t\text{-(BEDT-TTF)}_2(I_xBr_{1-x})_3 \text{ mainly}\\ \text{amorphous}_t\ \text{(BEDT-TTF)}/(I_xBr_{1-x})_3\end{cases}$$

In accordance with thermodynamic consideration:

$$I(\alpha'+\beta+\text{amorphous}):Br(\alpha'+\beta+\text{amorphous}) = 1:1$$
$$I(\alpha'_t+\beta_t+\text{amorphous}_t):Br(\alpha'_t+\beta_t+\text{amorphous}_t) = 1:1$$

In that case, the $x(\alpha')$, $x(\alpha'_t)$, and $x(\beta_t)$ values can be different. Previously, we also observed the decomposition of the (BEDT-TTF)$_2$I$_3$ nanocrystals under the film annealing during the MRDT third step. To prevent the loss of iodine and decomposition of the nanocrystals at the $\alpha \rightarrow \beta_t$ (BEDT-TTF)$_2$I$_3$ transition, we have annealed these BL-film samples in the presence of a small amount of I$_2$ vapors.

The same solid-state reactions can also accompany the $\alpha \rightarrow \beta$ and $\alpha' \rightarrow \beta$ transitions in the single crystals of the BEDT-TTF trihalide salts, but for those the loss of halogen in a remarkable amount was not observed.[9,18,19] It seems plausible that these speculative solid-state reactions proceeding in the surface layer of a solid are of a little importance for bulk single crystals but they can be crucial for the delicate BL-film's nanocrystals with a rich developed surface.

According to the Raman spectrum of sample **1,** the β_t-(BEDT-TTF)$_2$(I$_x$Br$_{1-x}$)$_3$ nanocrystals contain the set of bands due to the vibrations of thihalide anions such as I_3^- (121 cm^{-1}), I_2Br^- (140 cm^{-1}), and IBr_2^- (167 cm^{-1}). Unfortunately, the low-frequency Raman spectra of the other annealed BL-film samples were poor due to a luminescence appearing in the BL-films annealed. The reason for that is not clear.

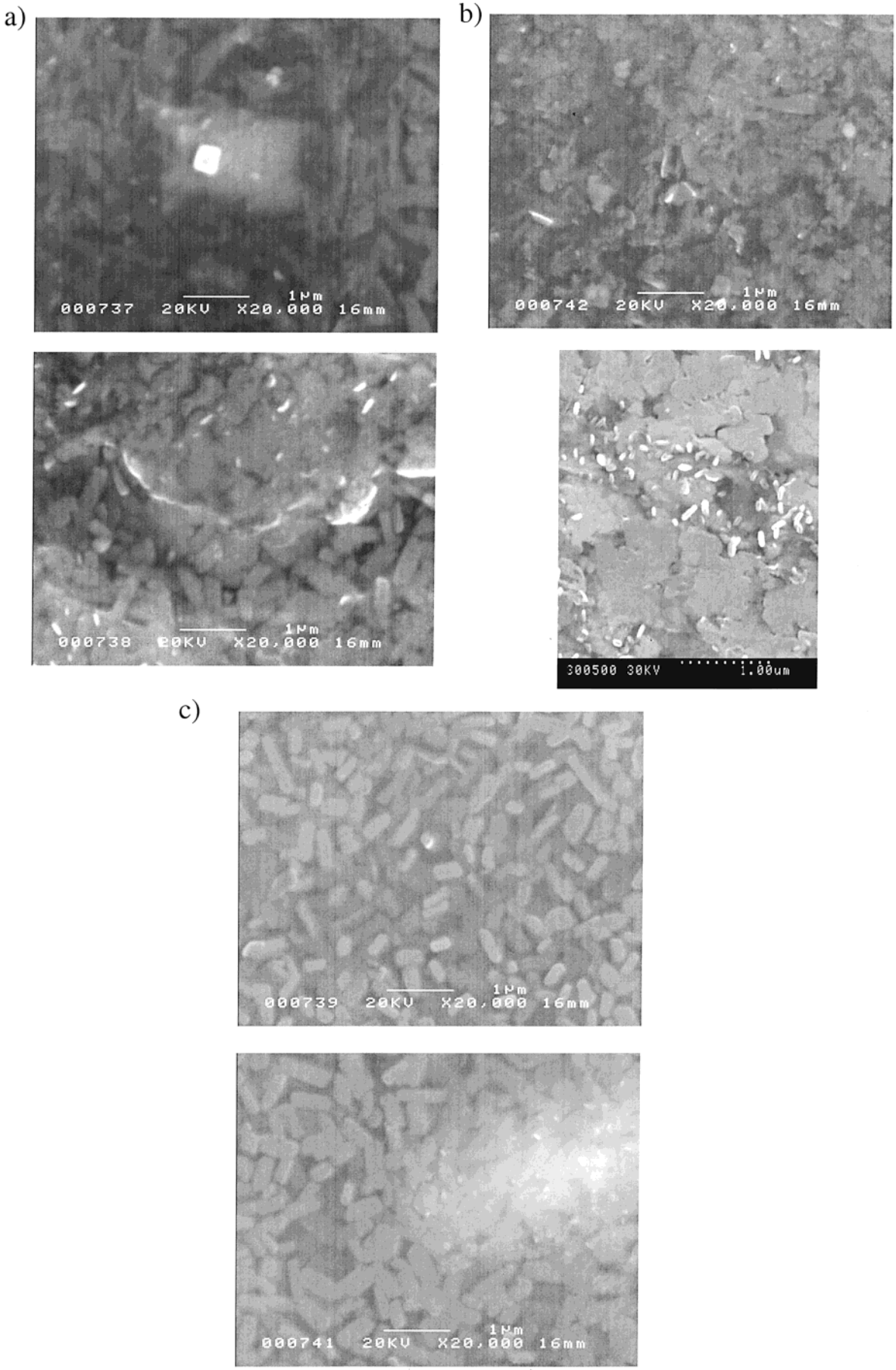

Figure 4. SEM images of BL-film samples (a) **1**, (b) **7**, and (c) **8** after the second (top) and third steps (bottom) of MRDT.

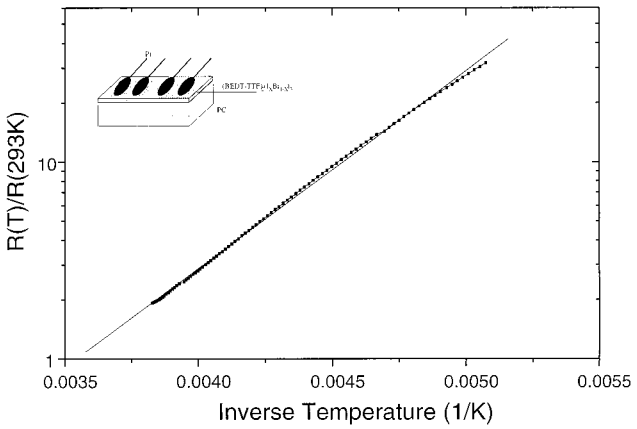

Figure 5. Normalized resistance of the conducting surface layer of the α′-(BEDT-TTF)$_2$(I_xBr_{1-x})$_3$ nanocrystals versus inverse temperature (sample **1** after the second step of MRDT). Inset shows the geometry of electrical contacts in a BL-film sample.

E. Textures of the Conducting Layers: SEM Studies. Taking into account that the quality of the nanocrystalline surface layer is very important in order to impart the electrical properties of molecular metals to the BL-films, we have studied the morphology (size, shape and orientation) of the (BEDT-TTF)$_2$(I_xBr_{1-x})$_3$ nanocrystals formed during the second and third step of MRDT. We have obtained the SEM images of samples **1**, **7**, and **8** (Figure 4). These samples were chosen as the typical BL-films containing the conducting surface layer of α′-(BEDT-TTF)$_2$(I_xBr_{1-x})$_3$ nanocrystals. According to the SEM images, all film samples contain a well oriented conducting layer: the largest faces of nanocrystals are parallel to the film surface. The texture of the α′-type conducting layer of sample **1** formed at the lowest F_{IBr} value consists of very small and poorly shaped nanocrystals (Figure 4a, top). By contrast, the nanocrystals of sample **8** are bigger and better shaped (Figure 4c, top). The textures of BL-films after annealing are shown in the bottom of Figure 4. The comparative analysis of these SEM images indicate that the textures of BL-films before and after annealing differ considerably: the β-type nanocrystals are better shaped and bigger than those of the initial α′-type nanocrystals.

F. Electrical Properties. To study the transport properties, rectangular pieces (≅1.5 × 0.5 mm^2) were cut out from the BL-film samples. The temperature dependence of the resistance of the BL-film samples was measured down to helium temperature. The typical temperature dependence of normalized resistance of the α′- and β_t-conducting layers is depicted in Figures 5 and 6, respectively. The resistance of the α′-conducting layers increases very strongly in decreasing temperature (Figure 5). When the temperature decreases from 300 to 175 K the resistance of the samples increases by a factor 100 with the activation energy value being equal to 0.2 eV, which is identical to that for the α′-(BEDT-TTF)$_2$IBr$_2$ single crystal. In contrast, the temperature dependence of resistance of the β_t-type conducting layers (samples **1**, **2**, and **5**−**7)** is metal-like down to nitrogen temperature, but at lower temperatures resistance starts to increase slightly. For example, the temperature dependence of resistance of sample **1** is presented in Figure 6 (curve a). The *R*(*T*) behavior of the annealed conducting layers which contain the β_t-(BEDT)$_2$(I_xBr_{1-x})$_3$ nanocrystals along with those of the α′-(BEDT-TTF)$_2$IBr$_2$ phase and N-salt is not metal-like: it increases with decreasing temperature (Figure 6, curve b), but all these samples are conductors down to helium temperature. Since the known β-type single crystals of BEDT-TTF with mixed trihalide anion[13] are

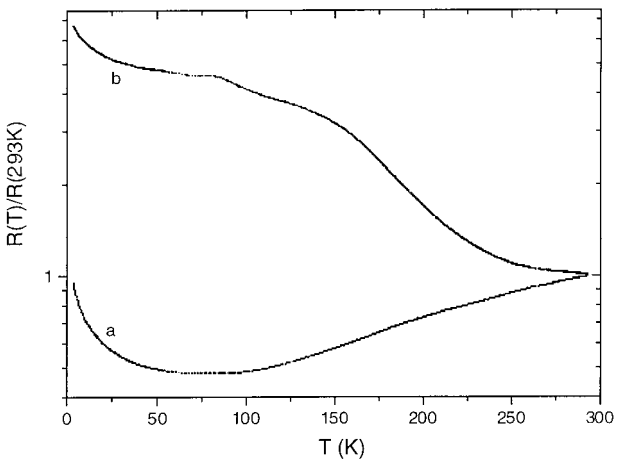

Figure 6. Typical temperature dependence of normalized resistance for different conducting surface layers containing the β_t-(BEDT-TTF)$_2$(I_xBr_{1-x})$_3$ nanocrystals as a main component: (a) film sample **1** and (b) film sample **8** (see text, Table 6).

metallic down to 1.5 K, we have expected that all the β_t-(BEDT-TTF)$_2$(I_xBr_{1-x})$_3$ conducting layers would show also the metal-like behavior of resistance down to helium temperature. However, the resistance of the β_t-type conducting layers of samples **1**, **2**, or **5**−**7** is not metal-like below nitrogen temperature. The transport properties of conducting layers in general depend on the conducting properties of the nanocrystals forming the layer as well as on the quality and the number of contacts between them. According to X-ray and SEM data the β_t-(BEDT-TTF)$_2$(I_xBr_{1-x})$_3$ nanocrystals are well "*c**" oriented and developed. Thus, one may conclude that the quality and/or number of contacts are not sufficient to form a continuous conducting layer revealing metal-like transport properties down to helium temperature.

4. Summary

A set of new conducting BL-films consisting of the polymeric PC/BEDT-TTF layer and thin surface layer of oriented (BEDT-TTF)$_2$(I_xBr_{1-x})$_3$ nanocrystals was prepared. All new transparent, flexible, and lightweight BL-films are conductors in a wide temperature region and some of them reveal metallic transport properties down to 80 K.

In the context of a thermodynamic approach, it was shown for the first time that the reduction of IBr should result in the formation of I_3^-, I_2Br^-, and IBr_2^- anions, giving the IBr_2^- species the major contribution. Ab initio calculations indicate that the contribution of these anions can depend on the polarity of the environment.

It was also shown that the α′ → β structural phase transition in the (BEDT-TTF)$_2$(I_xBr_{1-x})$_3$ nanocrystals takes place around 160−170 °C.

Acknowledgment. We are grateful to Dr. V. Laukhin and Prof. R. P. Shibaeva for useful discussions as well as to Dr. L. Buravov for help with dc-conductivity measurements.This work was supported by NATO (Project CRG.LG.974316), by DGI−Spain (BQU2000-1157), by Generalitat de Catalunya (2000 SGR-00114), by the Russian Foundation for Basic Research (Project 00-03-33200), by the Russian National Program "*Physics of Quantum and Wave Processes*", and by Polish State Committee for Scientific Research, Grant 7T08E06614p02. E.L. is grateful to Spanish Ministerio de Educacion y Cultura for Sabbatical at ICMAB (CSIC).

References and Notes

(1) Laukhina, E. E.; Merzhanov, V. A.; Pesotskii, S. I.; Khomenko, A. G.; Yagubskii, E. B.; Ulanski, J.; Kryszewski, M.; Jeszka, J. K. *Synth. Met*. **1995**, *70*, 797.

(2) Ulanski, J.; Kryszewski, M. In *The Encyclopedia of Advanced Materials*; Bloor, D., Brook, R. J., Fleming, M. C., Mahajan, S., Cahn, R. W., Eds.; Pergamon: Oxford, 1994; p 2301.

(3) Laukhina, E.; Tkacheva, V.; Shibaeva, R.; Khasanov, S.; Rovira, C.; Veciana, J.; Vidal-Gancedo, J.; Tracz, A.; Jeszka, J. K.; Sroczynska, A.; Wojciechowski, R.; Ulanski, J.; Laukhin, V. *Synth. Met.* **1999**, *102*, 1785.

(4) Jeszka, J. K.; Tracz, A. *Polym. Adv. Technol.* **1992**, *3*, 139.

(5) Williams, J. M.; Ferraro, J. R.; Thorn, R. J.; Carlson, K. D.; Geiser, U.; Wang, H. H.; Kini, A. M.; Whangbo, M.-H. *Organic Superconductors (Including Fullerenes): Synthesis, Structure, Properties, and Theory*; Prentice Hall: Englewood Cliffs, New Jersey, 1992.

(6) Horiuchi, S.; Yamochi, H.; Saito, G.; Jeszka, J. K.; Tracz, A.; Sroczyñska, A.; Ulanski, J. *Mol. Cryst. Liq. Cryst.* **1997**, *296*, 365.

(7) Ulanski, J.; Tracz, A.; Jeszka, J. K.; Laukhina, E.; Khomenko, A.; Polanowski, P.; Staerk, D.; Helberg, H. W. In *NATO ARW: Electrical and Related Properties of Organic Solids*; Munn, R. W., Kuchta, B., Miniewich, A., Ed.; Kluwer: Dordrecht, 1996; p 241.

(8) Laukhina, E. E.; Ulanski, J.; Khomenko, A. G.; Pesotskii, S. I.; Tkachev, V.; Atovmyan, L.; Yagubskii, E. B.; Rovira, C.; Veciana, J.; Vidal-Gancedo, J.; Laukhin, V. *J. Phys. I Fr.* **1997**, *7*, 1665.

(9) Baran, G. O.; Buravov, L. I.; Degtyarev, L. S.; Kozlov, M. E.; Laukhin, V. N.; Laukhina, E. E.; Onishchenko, V. G.; Pokhodnya, K. I.; Sheinkman, M. K.; Shibaeva, R. P.; Yagubskii, E. B. *Pis'ma Zh. Eksp. Teor. Fiz.* (USSR) **1986**, 44, 6, 293; *JETP Lett.* (U.S.A.) **1986**, *44*, 376 (English translation).

(10) Creuzet, F.; Creuzet, G.; Jerome, D.; Schweitzer, D.; Keller, H. J. *J. Phys. Lett.* **1985**, *46*, 1079.

(11) Frisch, M. J.; Trucks, G. W.; Schlegel, H. B.; Gill, P. M. W.; Johnson, B. G.; Robb, M. A.; Cheeseman, J. R.; Keith, T. A.; Peterson, G. A.; Montgomery, J. A.; Raghavachari, K.; Al-Laham, M. A.; Zakrzewski, V. G.; Ortiz, J. V.; Foresmen, J. B.; Peng, C. Y.; Ayala, P. Y.; Wong, M. W.; Andres, J. L.; Replogle, E. S.; Gomperts, R.; Martin, R. L.; Fox, D. J.; Binkley, J. S.; Defrees, D. J.; Baker, J.; Stewart, J. P.; Head-Gordon, M.; Gonzalez, C.; Pople, J. A. *Gaussian 94*, revision D.1; Gaussian, Inc.: Pittsburgh, PA, 1995.

(12) Wong, M. W.; Wiberg, K. B.; Frisch, M. J. *J. Am. Chem. Soc.* **1992**, *114*, 523.

(13) Laukhina, E. E.; Narymbetov, B. Zh.; Zorina, L. V.; Khasanov, S. S.; Rozenberg, L. P.; Shibaeva, R. P.; Buravov, L. I.; Yagubskii, E. B.; Avramenko, N. V.; Van, K. *Synth. Met.* **1997**, *90*, 101.

(14) Wojciechowski, R.; Ulanski, J.; Lefrant, S.; Faulques, E.; Laukhina, E.; Tkacheva, V. *J. Chem. Phys.* **2000**, *112*, 7634.

(15) Atkins, P. W. *Physical Chemistry*; Oxford University Press: New York, 1978.

(16) Shibaeva, R. P.; Kaminskii, V. F.; Linderman, S. V.; Yagubskii; E. B. *Sov. Phys. Crystallogr.* **1986**, *31*, 546 (English Translation).

(17) Sugai, S.; Saito, G. *Solid State Commun.* **1986**, *58*, 759.

(18) Avramenko, N. V.; Zvarykina, A. V.; Laukhin, V. N.; Laukhina, E. E.; Lubovskii, R. B.; Shibaeva,R. P. *JETP Lett.* **1988**, *48*, 472.

(19) Wang, H. H.; Carson, K. D.; Montgomery, L. K.; Schlueter, J. A.; Cariss, C. S.; Kwok, W. K.; Geiser, U.; Crabtree, G. W.; Williams, J. M. *Solid State Commun.* **1988**, *66*, 1113.